Loop engineering of an -1,3/4-L-fucosidase for improved synthesis of human milk oligosaccharides

Zeuner, Birgitte; Vuillemin, Marlene; Holck, Jesper; Muschiol, Jan; Meyer, Anne S.

Published in:
Enzyme and Microbial Technology

Link to article, DOI:
10.1016/j.enzmictec.2018.04.008

Publication date:
2018

Document Version
Peer reviewed version

Title: Loop engineering of an α-1,3/4-L-fucosidase for improved synthesis of human milk oligosaccharides

Authors: Birgitte Zeuner, Marlene Vuillemin, Jesper Holck, Jan Muschiol, Anne S. Meyer

PII: S0141-0229(18)30101-7
DOI: https://doi.org/10.1016/j.enzmictec.2018.04.008
Reference: EMT 9204

To appear in: *Enzyme and Microbial Technology*

Received date: 12-3-2018
Revised date: 18-4-2018
Accepted date: 22-4-2018

Please cite this article as: Zeuner Birgitte, Vuillemin Marlene, Holck Jesper, Muschiol Jan, Meyer Anne S.Loop engineering of an α-1,3/4-L-fucosidase for improved synthesis of human milk oligosaccharides.*Enzyme and Microbial Technology* https://doi.org/10.1016/j.enzmictec.2018.04.008

Loop engineering of an α-1,3/4-L-fucosidase for improved synthesis of human milk oligosaccharides

Birgitte Zeuner, Marlene Vuillemin, Jesper Holck, Jan Muschiol, Anne S. Meyer*

Center for Bioprocess Engineering, Department of Chemical and Biochemical Engineering, Technical University of Denmark, Building 229, DK-2800 Kgs. Lyngby, Denmark.

*Corresponding author: am@kt.dtu.dk

Graphical abstract

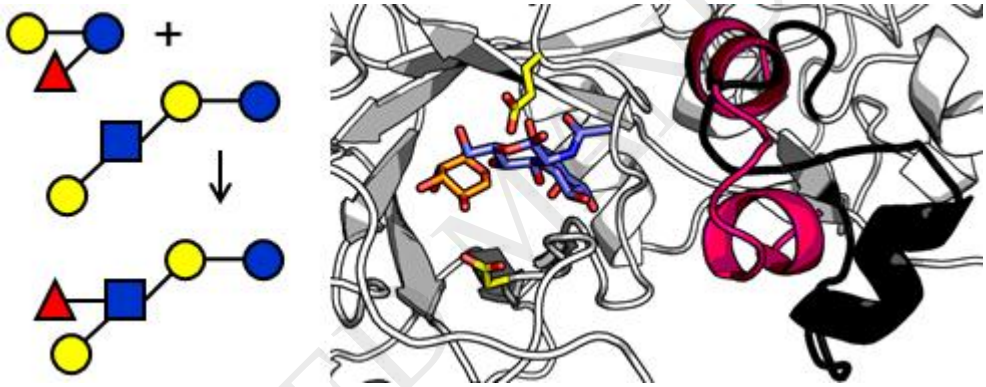

Highlights

- Targeted loop engineering of a GH29 fucosidase for improved transfucosylation
- 3-fold yield increase in the enzyme's conversion efficacy on the fucosyl donor
- Enzymatic synthesis of fucosylated human milk oligosaccharides LNFP II and LNFP III

Abstract

The α-1,3/4-L-fucosidases (EC 3.2.1.111; GH29) *Bb*AfcB from *Bifidobacterium bifidum* and *Cp*Afc2 from *Clostridium perfringens* can catalyse formation of the human milk oligosaccharide (HMO) lacto-

N-fucopentaose II (LNFP II) through regioselective transfucosylation of lacto-*N*-tetraose (LNT) with 3-fucosyllactose (3FL) as donor substrate. The current work exploits structural differences between the two enzymes with the aim of engineering *Bb*AfcB into a more efficient transfucosidase and approaches an understanding of structure-function relations of hydrolytic activity vs. transfucosylation activity in GH29. Replacement of a 23 amino acids long α-helical loop close to the active site of *Bb*AfcB with the corresponding 17-amino acid α-helical loop of *Cp*Afc2 resulted in almost complete abolishment of the hydrolytic activity on 3FL (6000 times lower hydrolytic activity than WT *Bb*AfcB), while the transfucosylation activity was lowered only one order of magnitude. In turn, the loop engineering resulted in an α-1,3/4-L-fucosidase with transfucosylation activity reaching molar yields of LNFP II of 39±2% on 3FL and negligible product hydrolysis. This was almost 3 times higher than the yield obtained with WT *Bb*AfcB (14±0.3%) and comparable to that obtained with *Cp*Afc2 (50±8%). The obtained transfucosylation activity may expand the options for HMO production: mixtures of 3FL and LNT could be enriched with LNFP II, while mixtures of 3FL and lacto-*N*-neotetraose (LNnT) could be enriched with LNFP III.

Abbreviations

2'FL: 2'-fucosyllactose; 3FL: 3-fucosyllactose; A:D: acceptor-to-donor ratio; *Bb*AfcB: α-1,3/4-L-fucosidase from *Bifidobacterium bifidum*; *Bi*AfcB: α-1,3/4-L-fucosidase from *Bifidobacterium longum* subsp. *infantis*; *Cp*Afc2: α-1,3/4-L-fucosidase from *Clostridium perfringens*; Fuc: fucose; GH: glycoside hydrolase; Gal: galactose; Glc: glucose; GlcNAc: *N*-acetylglucosamine; HMO: human milk oligosaccharide; LNT: lacto-*N*-tetraose; LNnT: lacto-*N*-neotetraose; LNFP: lacto-*N*-fucopentaose; Sia: sialic acid; WT: wild type.

Keywords: fucosidase, GH29, human milk oligosaccharides, protein engineering, transglycosylation

Introduction

Human milk oligosaccharides (HMOs) are soluble complex glycans which are present in human milk at concentrations of 5-15 g/L, often exceeding the concentration of protein thus being the third most abundant component in human milk. In the human colostrum, concentrations are even higher [1]. In contrast, HMOs are virtually absent from bovine milk, which is the basis of infant formula. Approx. 1% of the HMOs are adsorbed, while the majority is either metabolized by the gut microbiota of the infant or excreted in the faeces [2, 3]. HMOs function as prebiotics and antimicrobial agents in the gut of breastfed infants, and they further protect the infant against pathogens by functioning as soluble decoy receptors for pathogen adhesion as well as through a number of immunomodulating effects. HMOs may also be involved in infant brain development [1]. No single HMO has all these effects at once, suggesting why as many as 200 different HMO structures have been identified in human milk [4, 5].

Five monosaccharides, i.e. galactose (Gal), glucose (Glc), *N*-acetylglucosamine (GlcNAc), fucose (Fuc), and sialic acid (Sia) derivative *N*-acetyl-neuraminic acid, form the HMO building blocks. All HMO molecules have lactose (Gal-β1,4-Glc) at the reducing end can be elongated in β1,3- or β1,6-linkages by two different disaccharide moieties, namely Gal-β1,3-GlcNAc (type 1) or Gal-β1,4-GlcNAc (type 2). The HMO backbone can be further modified with Sia and/or Fuc substitutions [1, 5]. Among them, the fucosylated species are the most abundant – at least in breastmilk of approx. 80% of the population since the degree and type of HMO fucosylation are linked to the secretor and Lewis blood status group of the mother [6].

Several routes to production of HMOs *in vitro* exist, one of them being the use of glycosidases catalysing transglycosylation [7, 8, 9]. Advantages of glycosidases include easy expression, robustness, and the option of using inexpensive naturally occurring donor substrates. Indeed, the α-1,3/4-L-fucosidase *Bi*AfcB from *Bifidobacterium longum* subsp. *infantis* (EC 3.2.1.111) was recently shown to catalyse transfucosylation of the HMO core structure lacto-*N*-tetraose (LNT)

with another HMO, namely 3-fucosyllactose (3FL), as fucosyl donor leading to formation of lacto-*N*-fucopentaose II (LNFP II) [10] (Figure 1). For this WT enzyme, transfucosylation yields on 3FL ranged from 6% to 12% depending on the substrate concentration, but through elaborate engineering of *Bi*AfcB mutants transfucosylation yields on 3FL of up to 60% were achieved [10, 11]. We recently studied two WT α-L-1,3/4-fucosidases (EC 3.2.1.111) – *Bb*AfcB from *Bifidobacterium bifidum* and *Cp*Afc2 from *Clostridium perfringens:* In terms of their transfucosylation potential *Cp*Afc2 was superior to the *Bb*AfcB producing molar transfucosylation yields of up to 39% (on the donor 3FL) in production of LNFP II [12]. These α-L-fucosidases belong to the glycoside hydrolase family 29 subfamily B (GH29B) which comprises retaining α-L-fucosidases with high specificity for branched α-1,3/4-fucosylations [13]. In turn, GH29B α-1,3/4-L-fucosidases have also been shown to possess high regioselectivity in transfucosylation [10, 12].

When comparing the transfucosylation and hydrolytic activities of *Bb*AfcB and *Cp*Afc2 it was evident that *Cp*Afc2 had markedly higher transfucosylation activity than *Bb*AfcB using 3FL and LNT for formation of LNFP II, and that BbAfcB in turn had significantly higher hydrolytic activity on 3FL than *Cp*Afc2 [12]. Unfortunately, *C. perfringens* is a potential pathogen, so the use of an enzyme derived from this organisms for production of HMOs for infant formulae may be controversial. In contrast, *B. bifidum* is considered a beneficial probiotic microbe. Consequently, the current work set out to exploit any structural differences between the two GH29B α-1,3/4-L-fucosidases with the aim of engineering of *Bb*AfcB for improving its transfucosylation activity and/or reducing its hydrolytic activity. Comparison of homology models of *Bb*AfcB and *Cp*Afc2 with the crystal structure of the well-studied *Bi*AfcB, reveal that *Bb*AfcB and *Cp*Afc2 appear similar in terms of active site structure and substrate-interacting residues. However, the models of the active site region suggest that an α-helical loop on the side of the active site constitutes a major difference between *Bb*AfcB and *Cp*Afc2. Since the transsialylation yield of a sialidase from *Trypanosoma rangeli* could be significantly improved by replacing a loop near the active site with the corresponding loop of a native transsialidase from *T. cruzi* [14], a similar approach was pursued here: The identified α-helical loop in

*Bb*AfcB was replaced with that of *Cp*Afc2, hypothesizing that the shape of the loop in *Cp*Afc2 provide better shielding of the active site from the aqueous environment and that this feature could be transferred to *Bb*AfcB by loop engineering.

Materials & Methods

Chemicals

The fucosylated oligosaccharides 3-fucosyllactose (3FL), lacto-*N*-tetraose (LNT), lacto-*N*-neotetraose (LNnT), and lacto-*N*-fucopentaose V (LNFP V) were purchased from Elicityl Oligotech (Crolles, France). All other chemicals were purchased from Sigma-Aldrich (Steinheim, Germany).

Homology modelling

Structure homology models were prepared using the *Homology Modeling* function of YASARA Structure, version 16.9.23 (YASARA Biosciences GmbH, Vienna, Austria) [15].The program identified automatically the following template structures in structural databases: 4ZRX, 3UES, 3MO4, 2BER, 2X0Y for *Bb*AfcB and 4ZRX, 5K9H, 3EYP, 3RB5, 2OZN for *Cp*Afc2. For each of the templates up to 5 homology models were prepared by the program, which afterwards were automatically ranked. Based on the ranking a hybrid model was prepared by the program, which finally was equilibrated by molecular dynamics simulation using the YASARA macro md_refine without changes [16]. The refined models with the lowest energy were quality checked using QMEAN4 [17] and subsequently used for comparison with the *Bi*AfcB structure 3UET. All figures showing 3D structures were prepared using PyMol (The PyMOL Molecular Graphics System, Version 1.1 Schrödinger, LLC). Sequence alignments were made with MUSCLE 3.8 [18].

Cloning, expression and purification of α-L-fucosidases

The sequence of α-L-1,3/4-fucosidase *Bb*AfcB from *Bifidobacterium bifidum* JCM 1254 (GenBank BAH80310.1; EC 3.2.1.111) was slightly truncated and codon-optimized for expression in *Escherichia coli* previously [12]. The resulting pET22b+/*bbafcb* plasmid was used as a template for deletion of the encoded loop 759-AAYNDGVDKVSLKPGQMAPDGKL-781 and introduction of the new loop DIEKMKERENPTYLNNG originating from α-L-1,3/4-fucosidase *Cp*Afc2 from *Clostridium perfringens* ATCC 13124 (GenBank ABG83106.1; EC 3.2.1.111) [12, 19] by PCR using the forward primer 5'-AACCCGACCTATCTGAACAACGGCGGCAGCATGAGCAGCGTGCTGAGCGAG-3' and the reverse primer 5'-TTCACGTTCTTTCATTTTTTCGATATCTTGCGGGCTCCATTCGGTCTGACGCGCC-3' where underlined nucleotides correspond to the new loop sequence (Table A.1; Table A.2). The plasmid template was removed by DpnI digestion. After purification using Illustra GFX PCR DNA and Gel Band Purification kit (GE Healthcare, Chicago, IL, USA), the PCR product was phosphorylated using T4 polynucleotide kinase (Thermo Fisher Scientific, Waltham, MA, USA) at 37°C during 1 hour and ligated overnight at 16°C using T4 DNA ligase (Thermo Fisher Scientific, Waltham, MA, USA). The ligated PCR product was then transformed into competent *E. coli* DH5α cells, prepared with the Mix & Go *E. coli* Transformation kit (Zymo Research, Irvine, CA, USA). Plasmid was extracted using QIAprep Spin Miniprep kit (Qiagen, Hilden, Germany) and checked by sequencing (Macrogen Europe, Amsterdam, the Netherlands).

Expression and purification of *Bb*AfcB, *Bb*AfcB$_{mut}$, and *Cp*Afc2 were carried out in *E. coli* BL21 (DE3) as described previously [12]. Protein purity was confirmed by SDS-PAGE and protein concentration was determined with the BCA Protein Assay Kit (Thermo Fisher Scientific, Waltham, MA, USA) using bovine serum albumin (BSA) standards.

Hydrolytic activity and HPAEC-PAD analysis

Hydrolytic activity was determined for *Bb*AfcB, *Bb*AfcB$_{mut}$, and *Cp*Afc2 using 0.1 mM 3FL in 50 mM buffer (acetate buffer pH 5.5 for *Bb*AfcB and *Bb*AfcB$_{mut}$ according to the pH optimum of BbAfcB established by Ashida et al. [20], and phosphate buffer pH 7.0 for *Cp*Afc2 according to the pH

optimum for CpAfc2 [19]) and enzyme concentrations between 0.005 µM and 5 µM. Negative controls without enzyme were included. All reactions took place at 40°C, were monitored for up to 20 min (180 min for *Bb*AfcB$_{mut}$), and stopped by mixing a sample 1:1 with 1 M Na_2CO_3. The amounts of substrate and hydrolysis products were quantified by high-performance anion exchange chromatography with pulsed amperometric detection (HPAEC-PAD). Specific hydrolytic activity was defined as µmol of product released per minute (U) per µmol of enzyme.

Enzyme stability at 40°C was determined by incubation of the fucosidases in the reaction buffer at 40°C followed by assessment of their remaining hydrolytic activity after 0, 1, 3, 5, 12, and 24 hours of incubation as described above.

HPAEC-PAD analysis was carried out on a Dionex ICS3000 system (Dionex Corp., Sunnyvale, CA, USA) using a CarboPac™ PA1 (4 mm x 250 mm) analytical column equipped with a CarboPac™ PA1 (4 mm x 50 mm) guard column (Dionex Corp., Sunnyvale, CA, USA) and a flow rate of 1 mL/min at 25°C. The eluent system comprised MilliQ water (A), 500 mM NaOH (B), and 500 mM NaOAc with 0.02% (w/v) NaN_3 (C). After enzymatic hydrolysis, 3FL was quantified by isocratic elution at 90:10:0 (% A:B:C) for 20 min using external standards of L-fucose, lactose, and 3FL. Strongly retained anions were washed from the column by elution with 10:10:80 (% A:B:C) for 5 min followed by re-equilibration of the column at 90:10:0 (% A:B:C) for 10 min.

Transfucosylation activity and LC-ESI-MS analysis

For transfucosylation of LNT and LNnT, 3FL was used as donor substrate for reactions catalysed by *Bb*AfcB, *Bb*AfcB$_{mut}$ and *Cp*Afc2. Enzyme concentration was 0.5 µM and reaction took place at 40°C for up to 24 hours in 100 mM buffer (acetate buffer pH 5.5 for *Bb*AfcB and *Bb*AfcB$_{mut}$, phosphate buffer pH 7.0 for *Cp*Afc2). Reactions were terminated by heating at 99°C for 15 min. For reactions with an acceptor-to-donor ratios (A:D) of 10, donor substrate (3FL) concentration was 10 mM and acceptor substrate (LNT or LNnT) concentration was 100 mM. For reactions with an A:D of 1, concentrations of donor and acceptor substrates were 20 mM. Additional experiments were conducted with *Bb*AfcB

and *Bb*AfcB$_{mut}$ at the same conditions (reaction time up to 60 min) using A:Ds of 2 (10 mM 3FL and 20 mM LNT) and 5 (20 mM 3FL and 100 mM LNT). Transfucosylation products were identified and quantified by liquid chromatography electrospray ionization mass spectrometry (LC-ESI-MS) using an external LNFP V standard. Transfucosylation yields were calculated as molar yields based on the donor substrate 3FL, i.e. the percentage of LNFP formed compared to the initial 3FL concentration. Initial transfucosylation rates were calculated as mM LNFP formed per min of reaction over the time where the product formation curve was linear (2 min for *Bb*AfcB, 5 min for *Cp*Afc2, and 20-30 min for *Bb*AfcB$_{mut}$).

Identification and quantification of LNFP transfucosylation products were performed by LC-ESI-MS on an Amazon SL iontrap (Bruker Daltonics, Bremen, Germany) coupled to an UltiMate 3000 UHPLC from Dionex (Sunnyvale, CA, USA) equipped with a porous graphitized carbon column (Hypercarb PGC, 150 mm × 2.1 mm, 3 µm; Thermo Fisher Scientific, Waltham, MA, USA) as described previously [12]. LNFP isomers LNFP II, LNFP III, and LNFP V were identified from MS^2 fragmentation patterns [21].

Statistics

One-way ANOVA for determination of statistical significance was performed with JMP®, version 13.0.0 (SAS Institute Inc., Cary, NC, USA). Statistical significance was established at $p < 0.05$.

Results

Homology modelling

The homology models of *Bb*AfcB and *Cp*Afc2 were inspected visually and their quality was checked using the QMEAN4 Z-score [17]. The model for *Bb*AfcB showed a dimeric structure, but since there was no significant difference in between the two monomers it was decided to continue with only one of them. The catalytic domains for both models showed the expected $(\beta/\alpha)_8$-barrel, though one of

the β-strands was not modelled as such (Figure A.1). However, aligning the models with the crystal structures of *Bi*AfcB (3UET) [22] and another GH29B member, namely α-L-1,3/4-fucosidase BT2192 from *Bacteroides thetaiotaomicron* (4OZO) [23], revealed that even in the crystal structure this part of the barrel was not a perfect β-strand; thus, this could be a natural feature of these enzymes. The QMEAN4 *Z*-scores for the full-length models of *Bb*AfcB and *Cp*Afc2 were -2.65 and -2.61, respectively (Figure A.2). Deleting the C-terminal non-catalytic domain for the quality check improved the Z-score for *Bb*AfcB only marginally (-2.51), but for *Cp*Afc2 the score significantly improved to -0.62 (Figure A.2). The low quality score for the *Bb*AfcB model might be caused by the long single α-helices present, which especially influence the packing check negatively. However, since the model of the catalytic domain for *Cp*Afc2 was of good quality, the models were used to identify potential targets to engineer *Bb*AfcB for improved transglycosylation performance.

Based on inspection of the homology models and comparison to the well-studied crystal structure of *Bi*AfcB, it was evident that they share all substrate-interacting residues in terms of position in the three-dimensional structure (Figure A.1; Figure A.3; Table A.3). However, *Cp*Afc2 featured an α-helical loop region on the side of the active site, approx. 13 Å from the substrate. In *Bb*AfcB, the major part of this α-helical loop was further away and more disordered (Figure 2) and in *Bi*AfcB it was even found to be a large disordered structure, because the structure of this loop could not be determined (Figure A.3). The most significant structural difference in the compared structures was this loop region, which was moreover found to be highly variable in the three sequences. Hence, the hypothesis behind the current work was that replacement of the loop sequence in *Bb*AfcB with that of *Cp*AfcB, would improve the transfucosylation ability of *Bb*AfcB by inducing a better shielding of the active site from the aqueous environment. This hypothesis was further supported by inspection of the surface representation of the aligned models, in which it became obvious that especially R266 in the *Cp*Afc2-loop might indeed shield the active site of *Bb*AfcB, even though there is still room for water molecules in the active site (Figure A.4).

To define the exact parts of the loop in *Bb*AfcB to be exchanged with the one from *Cp*Afc2 the homology models were aligned in PyMol and inspected visually. To minimize the risk of losing the correct foldability and also a possible dimerization of *Bb*AfcB, the starting and end points of the loops to be exchanged were carefully selected based on backbone alignment. The backbones of the amino acid residues A759 in *Bb*AfcB and D259 in *Cp*Afc2 aligned well, so these residues were defined as starting points of the loops to be exchanged (Figure A.1). Although true backbone alignment was not achieved until L799 in *Bb*AfcB and S280 in *Cp*Afc2, detailed inspection of the modelled loop structures revealed that G782 of *Bb*AfcB and E276 of *Cp*Afc2 aligned well enough, so that these two positions were defined to terminate the loops to be exchanged (Figure A.1). This led to the final definition of the loop 759-AAYNDGVDKVSLKPGQMAPDGKL-781 in *Bb*AfcB to be exchanged with the loop 259-DIEKMKERENPTYLNNG-275 from *Cp*Afc2.

Expression of recombinant α-1,3/4-L-fucosidases

*Bb*AfcB, *Bb*AfcB$_{mut}$ loop mutant, and *Cp*Afc2 were successfully expressed in *E. coli* BL21 (DE3) cells using LB medium. After Ni^{2+} affinity chromatography purification and desalting by gel filtration expression levels reached 24, 23, and 38 mg of purified enzyme per litre of culture, respectively. SDS-PAGE analysis showed that all purified extracts were satisfactorily pure (Figure A.5).

Hydrolytic activity

The hydrolytic activities of *Bb*AfcB and *Cp*Afc2 on 3FL were similar to the previously reported values [12]: 18 U/µmol enzyme for *Cp*Afc2 and 59 U/µmol enzyme for *Bb*AfcB. However, for *Bb*AfcB$_{mut}$ the hydrolytic activity on 3FL was practically non-existent: 0.01 U/µmol enzyme, i.e. 6000 times lower than the WT enzyme (Table 1).

Transfucosylation activity

Transfucosylation activity of *Bb*AfcB$_{mut}$, *Bb*AfcB, and *Cp*Afc2 was monitored for 3 hours using 3FL as fucosyl donor and LNT or lacto-*N*-neotetraose (LNnT) as acceptors. The acceptor-to-donor ratios (A:D) were either 10 (acceptors 100 mM LNT or LNnT and donor 10 mM 3FL) or 1 (20 mM of each substrate). For WT *Bb*AfcB, maximum levels of LNFP II and LNFP III were obtained after 2 minutes of reaction, which was the shortest reaction time measured; after this, product levels decreased to 0 within 2 hours of reaction (Figure 3). At A:D 10, the maximum yield of LNFP II was 14%, whereas it was 3.3% for LNFP III (Figure 3; Table 2). For *Cp*Afc2, the transient maxima were reached after 30 minutes and yields were 50% for LNFP II and 17% for LNFP III at A:D 10 (Figure 3; Table 2). For *Bb*AfcB$_{mut}$, no transient maxima were observed within 3 hours of reaction (Figure 3). Instead, maximum yields were obtained after 3 hours reaching 39% for LNFP II and 11% for LNFP III on the 3FL donor at A:D 10 (Figure 3, Table 2).

Interestingly, the highest apparent initial transfucosylation rates were obtained with *Bb*AfcB, being approx. 1.5 times higher than those of *Cp*Afc2 at A:D 10 and 2-3 times higher at A:D 1 (Table 2). In comparison, initial transfucosylation rates were approx. one order of magnitude lower for *Bb*AfcB$_{mut}$ compared to the two WT enzymes (Table 2).

Additional samples were taken after 24 hours of reaction in order to investigate the degree of product hydrolysis. For both WT enzymes *Bb*AfcB and *Cp*Afc2, product degradation was complete after 24 hours (Table 2). However, for *Bb*AfcB$_{mut}$ no significant decrease in LNFP II levels were observed, whereas the level of LNFP III did decrease at A:D 10 though not at A:D 1 (Table 2). After incubation at 40°C for 24 hours in reaction buffer, the remaining activities were 77%, 100%, and 81% for *Bb*AfcB$_{mut}$, *Bb*AfcB, and *Cp*Afc2, respectively. For *Bb*AfcB$_{mut}$, a half-life of 66 hours was determined, whereas it was 82 hours for *Cp*Afc2.

In addition to LNFP II, small amounts of LNFP V (i.e. the LNFP isomer where Fuc is α1,3-linked to the reducing end Glc moiety of LNT) were detected in the reaction with 3FL and LNT catalysed by *Bb*AfcB$_{mut}$ (Figure A.6). After 3 hours of reaction, the yield of LNFP V was 5% at A:D 10 and 0.6% at

A:D 1 corresponding to 11% and 5% of the total transfucosylation yield, respectively. No LNFP V was detected in the reaction catalysed by *Cp*Afc2, and for WT *Bb*AfcB yields never exceeded 0.5%.

In most cases, significantly higher yields were obtained at A:D 10 compared to A:D 1 (Table 2). To further explore the influence of A:D and substrate concentration, *Bb*AfcB and *Bb*AfcB$_{mut}$ were employed at A:D 1, 2, 5, and 10 combining two different donor concentrations (10 mM and 20 mM) with two different acceptor concentrations (20 mM and 100 mM) (Table 3; Figure 4). In this way, the effect of donor concentration, acceptor concentration, and their molar ratio (A:D) on product formation and yield were investigated simultaneously. In all cases, the same enzyme showed similar reaction progress over time independent of the A:D and substrate concentration employed (Figure 4). To clearly investigate the effect of both parameters, initial transfucosylation rates were divided by the initial 3FL concentration (10 or 20 mM). Doing so, almost identical values were obtained for reactions with identical LNT acceptor concentrations (Table 3). In turn, the initial transfucosylation rates increased 4 times for *Bb*AfcB$_{mut}$ and CpAfc2 when the acceptor concentration was increased 5 times (Table 3). For *Bb*AfcB this was not the case, as a 5-fold increase in acceptor concentration led to a 1.5-fold increase in initial transfucosylation rate only (Table 3). Similar trends were observed for maximum LNFP II yields obtained within 60 minutes of reaction (Table 3).

Discussion

Examples of loop deletions exist as a strategy for improving transglycosylation activity in microbial enzymes with polymeric substrates, e.g. xyloglucan endo-hydrolases (using xyloglucan endo-transglycosylases as template) [24] and α-amylases (using cyclodextrin glucanotransferases as template) [25]. However, point mutations – single or multiple – in and around the active site comprise by far the most pursued strategy for exoglycosidases [26-29], and is also the only protein engineering strategy previously used on GH29 α-L-fucosidases [10, 11, 22, 30]. However, for a sialidase from *Trypanosoma rangeli* it was shown that exchanging a loop of seven amino acids

approx. 10 Å from the active site with the seven amino acids found in the corresponding loop in the native transsialidase from *Trypanosoma cruzi* significantly improved transsialylation yields [14]. The loop mutation mainly reduced the hydrolytic activity, whereas it had little effect on the transsialylation rate [29]. On a more general level, the interest in the flexible loop regions and their impact on enzyme function is increasing and as a consequence engineering of loop regions is becoming a more commonly pursued strategy [31].

Enzymes of the GH29 family have a $(\beta/\alpha)_8$ or TIM-barrel-like fold (although one α-helix may be missing), where all the conserved active site residues are on the catalytic βα-loops, i.e. the loops that follow after the β-strands [32, 33]. The active sites of GH29 members exhibit a pocket topology which is common for exoglycosidases [34]. Conservation is strict among the ligand interacting residues inside the active site pocket, but there is large diversity in the overall shape due to variation in the loops surrounding the active site [32]. Crystal structures provided evidence that some of the loops undergo conformational changes upon substrate binding and that at least two of the loops take part in the catalytic process in *Bi*AfcB (Table A.3) [22]. Thus, the loops near the active site could indeed be an interesting target for α-L-fucosidase engineering. The loop targeted in the current work appears highly flexible as it was disordered and not properly crystallized in the crystal structure of *Bi*AfcB (Table A.3) [22]. In the $(\beta/\alpha)_8$-barrel structure, mutations in the catalytic βα front loops often do not cause stability issues since they are separated in space by the central barrel structure from the αβ back loops, which confer stability [33, 35]. This separation could give functional versatility in enzymes with $(\beta/\alpha)_8$-barrel-like folds, and the $(\beta/\alpha)_8$-barrel is therefore considered an ideal scaffold for rational design of novel enzyme activities [33, 35, 36]. Indeed, several reports exist on loop grafting, i.e. replacing βα-loops from one enzyme of the $(\beta/\alpha)_8$-barrel fold class with those from another, for transferring substrate specificity and function although not yet for transglycosylation purposes [36, 37].

The loop mutation in the *T. rangeli* sialidase introduced a change in net charge of +3 and it was hypothesized that it altered the water network in the active site [14]. In the current work, a 23-

amino acid α-helical loop with a net charge of 0 was replaced by a 17-amino acid α-helical loop with a net charge of -1. Rather than altering the water network it was hypothesized that this would lead to better shielding of the active site pocket from the surrounding aqueous environment, thus reducing the competing hydrolytic activity. A closed active site topology, a hydrophobic entrance to the active site, or obstruction of catalytic water channels to exclude water from the active site have all been shown to have positive effects on transglycosylation for GH33 sialidases, GH1 β-glucosidases, and GH13 neopullulanase [38-42]. Indeed, the study of the homology models of *Cp*Afc2 and *Bb*AfcB suggested that the α-helical loop in *Cp*Afc2 could have a more shielding effect than the more open and disordered loop found in *Bb*AfcB, although the models indicate that there is still ample room for water molecules in the active site (Figure 2; Figure A.4). While these were indeed models – and the corresponding loop in *Bi*AfcB so flexible that it could not be crystallized [22] – the results emphasize that the exchange of the loop in *Bb*AfcB with that of *Cp*Afc2 did indeed have a major effect on the transfucosylation performance of *Bb*AfcB, mainly by almost completely abolishing its hydrolytic activity while maintaining an initial transfucosylation rate which was approx. one order of magnitude lower than those observed in WT *Bb*AfcB and *Cp*Afc2 (Table 1; Table 2; Table 3). A drop in activity rate is often observed in glycosidases engineered for improved transglycosylation, especially when mutations are in the negative subsite (i.e. the donor binding site) and/or when more than one amino acid is substituted [27, 28]. Exchange of a loop in the *T. rangeli* sialidase with the corresponding one of *T. cruzi* transsialidase also reduced the hydrolytic activity significantly, indicating that this strategy – which is similar to the one employed here – particularly targets the undesirable hydrolytic activity [14, 29]. The loop mutation did not influence the expression levels of recombinant *Bb*AfcB and *Bb*AfcB$_{mut}$ in *E. coli*, which were similar. Enzyme stability at extended reaction times was slightly influenced by the loop mutation: whereas *Bb*AfcB retained full activity after 24 hours of incubation at 40°C, the remaining activity of *Bb*AfcB$_{mut}$ was 77% and thus more similar to that of *Cp*Afc2, which was 81%. However, 77% is an appreciable remaining activity and it should be feasible to run the reaction

past 24 hours in order to obtain higher transfucosylation yields with *Bb*AfcB$_{mut}$ at A:D 1. At A:D 10, maximum yields were obtained within 24 hours of reaction (Table 2).

For glycosidase-catalyzed transglycosylation, product maxima are often transient due to hydrolysis [8]. Interestingly, despite having the highest initial transfucosylation rate, *Bb*AfcB gave the lowest transfucosylation product yields. From this, it is evident that transfucosylation rate is not the only important factor. Indeed, when employing glycosidases for transglycosylation, hydrolytic rates on substrate as well as on product are just as important as the transglycosylation rate in determining the maximum transglycosylation yield (Table 2; Figure 3). The fact that maximum product levels were obtained at the shortest measured reaction time with *Bb*AfcB (Figure 3) is indeed linked to the fact that this enzyme had significantly higher hydrolytic activity than *Bb*AfcB$_{mut}$ and *Cp*Afc2 (Table 1). For *Cp*Afc2 the transient maximum occurred at a later stage (30 min; Figure 3), whereas the product hydrolysis was limited for *Bb*AfcB$_{mut}$, which had very low hydrolytic activity on 3FL compared to the two WT enzymes (Figure 3; Table 1). As discussed above, the transfucosylation activity was also approx. one order of magnitude lower, but due to the dramatic decrease in product hydrolysis, appreciable levels of LNFP II and LNFP III were reached with *Bb*AfcB$_{mut}$ (Table 2). While *Cp*Afc2 produced even higher yields at A:D 10, the yields were similar with *Cp*Afc2 and *Bb*AfcB$_{mut}$ at A:D 1 (Table 2).

It is well established that both substrate concentration and A:D affect transglycosylation rates and yields [8]. The transfucosylation data on LNT with 3FL as donor catalyzed by *Bb*AfcB or *Bb*AfcB$_{mut}$ suggested that the progress and mechanism of the reactions were independent of A:D and substrate concentration (Figure 4). Dividing initial transfucosylation rates and transfucosylation yields by the initial donor substrate concentration revealed similar values for reactions with identical acceptor concentrations, indicating that the effect of donor substrate concentration was linear in this range (Table 3). Analogously, there was a clear effect of the acceptor concentration: For *Bb*AfcB$_{mut}$ a 4-fold higher initial rate and a 5.5-fold higher yield was obtained when the acceptor concentration was increased 5 times (Table 3). A similar trend was observed for *Cp*Afc2, although the increase in

yield was only 3-fold (Table 3). For WT *Bb*AfcB, increases in rate and yield were only 1.5-fold (Table 3). Most likely, initial transfucosylation rates were heavily influenced by the large hydrolytic activity of this enzyme, and the effect of A:D was therefore not as evident (Table 1; Table 3). Indeed, the transient maximum was passed within the first two minutes of reaction, and the initial transfucosylation rate and maximum yield may therefore be higher than established here (Figure 4).

The transfucosylation activity was tested on two different HMO acceptor substrates of equal size, namely LNT and LNnT which differ only in the linkage between the non-reducing Gal moiety and GlcNAc (β1,3 in LNT and β1,4 in LNnT; Figure 1). Both were used as substrates for transfucosylation with 3FL, resulting in formation of HMO pentaose structures LNFP II and LNFP III, respectively, as identified by LC-ESI-MS/MS (Figure 1). However, for WT α-1,3/4-L-fucosidases *Bb*AfcB and *Cp*Afc2 initial transfucosylation rates were 4-5 times higher on LNT compared to LNnT (Table 2). For *Bb*AfcB$_{mut}$ the difference was more moderate, the initial rate being only 2 times higher for LNT (Table 2). Similarly, maximum yields were higher for LNFP II than for LNFP III, the difference between the enzymes being less distinct (Table 2). The slightly larger preference for LNnT observed in *Bb*AfcB$_{mut}$ compared to the WT α-1,3/4-L-fucosidases could be linked to the less strict regioselectivity observed for the engineered enzyme in the transfucosylation of LNT, where formation of minor amounts of LNFP V was observed. Although the crystal structure of orthologue *Bi*AfcB indicates that the reducing end of LNFP II protrudes from the enzyme, while the non-reducing end Gal moiety is buried in the active site pocket (Figure 2; Figure A.1) [22], the formation of LNFP V indicates that *Bb*AfcB$_{mut}$ must be able to accommodate LNT in a reverse manner. This may be a result of the loop engineering since only negligible amounts of LNFP V were observed in reactions catalyzed by WT *Bb*AfcB. However, no LNFP V was observed in reactions catalysed by *Cp*Afc2, indicating that it was not the loop as such, but rather its effect on *Bb*AfcB$_{mut}$. LNFP V is present in human milk, albeit only in very small amounts [43].

The only previously reported engineering of *Bb*AfcB is its transformation into an α-L-fucosynthase, giving an LNFP II yield of 41% when using 34 times more enzyme than in the current

work [22]. While this strategy is appealing due to its simple, generic nature, especially α-glycosynthases struggle with low donor substrate stability [22, 44]. GH29B α-1,3/4-L-fucosidases are particularly appealing in terms of engineering for improved transfucosylation activity – and for use in transfucosylation in general – since they appear to maintain their high regioselectivity in the transfucosylation reaction, while the GH29A α-L-fucosidases often do not [10, 12, 22]. So far, the only other example of engineering of a GH29B α-1,3/4-L-fucosidase is the extensive work on *Bi*AfcB [10, 11]. Together with these results, the current work emphasizes the potential of protein engineering for improved transfucosylation performance among GH29B enzymes, as well as for targeted loop engineering in general. In addition, the work highlights how the competition between transglycosylation and hydrolysis rates governs glycosidase-catalysed transglycosylation and why reduction of hydrolytic activity is an important strategy in transglycosidase engineering.

The use of glycosidase-catalysed transglycosylation represents one strategy for *in vitro* production of HMOs [7, 8]. An alternative strategy for *in vitro* HMO production is the use of prokaryotic fucosyltransferases; however, their expression is challenging and their use requires a multi-enzyme setup for regeneration of the required expensive substrate GDP-L-fucose [9]. For fairly simple HMO structures, fermentation of engineered *Escherichia coli* appears to be a viable strategy. For instance, HMOs including 2'-fucosyllactose (2'FL), 3FL, LNT, and LNnT have been produced by engineered *E. coli* with yields generally around 10 g/L [7, 45-47]. However, for more complex structures such as LNFPs yields are generally much lower and only LNFP I and LNFP III have been reported as fermentation products with yields below 1 g/L [48, 49]. A process combining fermentation products with regioselective enzymatic transfucosylation catalysed by α-L-fucosidases could lead to a mixture of 3FL and LNT enriched with LNFP II, which is the seventh most abundant HMO in general and the second most abundant HMO in non-secretor milk [6].

Being of lactic acid bacterial origin, the use of engineered *Bb*AfcB for production of human milk oligosaccharides may be a more suitable strategy than employing *Cp*Afc2 from pathogenic *C. perfringens.* The newly obtained transfucosylation activity could be exploited to expand the

complexity of HMO production: mixtures of 3FL and LNT – e.g. of fermentation origin – could be enriched with LNFP II, while mixtures of 3FL and LNnT could be enriched with LNFP III.

Funding

This work was supported by the Danish Council for Independent Research [grant number 5054-00046] (grant to BZ); and by the H.C. Ørsted COFUND postdoc fellowship programme (grant to MV).

References

[1] L. Bode, Human milk oligosaccharides: Every baby needs a sugar mama, Glycobiology 22 (2012) 1147-1162.

[2] M.B. Engfer, B. Stahl, B. Finke, G. Sawatzki, H. Daniel, Human milk oligosaccharides are resistant to enzymatic hydrolysis in the upper gastrointestinal tract, Am. J. Clin. Nutr. 71 (2000) 1589-1596.

[3] S. Albrecht, H.A. Schols, E.G.H.M van den Heuvel, A.G.J. Voragen, H. Gruppen, Occurrence of oligosaccharides in feces of breast-fed babies in their first six months of life and the corresponding breast milk, Carbohydr. Res. 346 (2011) 2540-2550.

[4] M.R. Ninonuevo, Y. Park, H. Yin, J. Zhang, R.E. Ward, B.H. Clowers, J.B. German, S.L. Freeman, K. Killeen, R. Grimm, C.B. Lebrilla, A strategy for annotating the human milk glycome, J. Agric. Food Chem. 54 (2006) 7471-7480.

[5] X. Chen, Human milk oligosaccharides (HMOS): structure, function, and enzyme-catalyzed synthesis, Adv. Carbohydr. Chem. Biochem. 72 (2015) 113-190.

[6] C. Kunz, C. Meyer, Y.C. Collado, L. Geiger, Y. Garcia-Mantrana, Z. Bertua-Rios, Z. Martinez-Costa, C. Borsch, S. Rudloff, Influence of gestational age, secretor, and Lewis blood group status on the oligosaccharide content of human milk, J. Pediatr. Gastroenterol. Nutr. 64 (2017) 789-798.

[7] G.A. Sprenger, F. Baumgärtner, C. Albermann, Production of human milk oligosaccharides by enzymatic and whole-cell microbial biotransformations, J. Biotechnol. 258 (2017) 79-91.

[8] B. Zeuner, C. Jers, J.D. Mikkelsen, A.S. Meyer, Methods for improving enzymatic trans-glycosylation for synthesis of human milk oligosaccharide biomimetics, J. Agric. Food Chem. 62 (2014) 9615-9631.

[9] B. Petschacher, B. Nidetzky B, Biotechnological production of fucosylated human milk oligosaccharides: Prokaryotic fucosyltransferases and their use in biocatalytic cascades or whole cell conversion systems, J. Biotechnol. 235 (2016) 61-83.

[10] A. Saumonneau, E. Champion, P. Peltier-Pain, D. Molnar-Gabor, J. Hendrickx, V. Tran, M. Hederos, G. Dekany, C. Tellier, Design of an α-L-transfucosidase for the synthesis of fucosylated HMOs, Glycobiology 26 (2016) 261-269.

[11] E. Champion, A. Vogel, S. Bartsch, G. Dekany, Mutated fucosidase, Patent WO2016/063261 A1 (2016) April 28.

[12] B. Zeuner, J. Muschiol, J. Holck, M. Lezyk, M.R. Gedde, C. Jers, J.D. Mikkelsen, A.S. Meyer, Substrate specificity and transfucosylation activity of GH29 α-L-fucosidases for enzymatic production of human milk oligosaccharides, New Biotechnol. 41 (2018) 34-45.

[13] H. Sakurama, E. Tsutsumi, H. Ashida, T. Katayama, K. Yamamoto, H. Kumagai, Differences in the substrate specificities and active-site structures of two α-L-fucosidases (glycoside hydrolase family 29) from *Bacteroides thetaiotaomicron*, Biosci. Biotechnol. Biochem. 76 (2012) 1022-1024.

[14] C. Jers, M. Michalak, D.M. Larsen, K.P. Kepp, H. Li, Y. Guo, F. Kirpekar, A.S. Meyer, J.D. Mikkelsen, Rational design of a new *Trypanosoma rangeli* sialidase for efficient sialylation of glycans, PLOS One 9 (2014) e83902.

[15] E. Krieger, G. Vriend, YASARA View – molecular graphics for all devices – from smartphones to workstations, Bioinformatics 30 (2014) 2981-2982.

[16] E. Krieger, T. Darden, S.B. Nabuurs, A. Finkelstein, G. Vriend, Making optimal use of empirical energy functions: Force-field parameterization in crystal space, Proteins: Struct., Funct., Bioinf. 57 (2004) 678–683.

[17] P. Benkert, S.C.E. Tosatto, D. Schomburg, QMEAN: A comprehensive scoring function for model quality assessment, Proteins: Struct., Funct., Bioinf. 71 (2008) 261-277.

[18] R.C. Edgar, MUSCLE: multiple sequence alignment with high accuracy and high throughput, Nucleic Acids. Res. 32 (2004) 1792-1797.

[19] S. Fan, H. Zhang, X. Chen, L. Lu, L. Xu, M. Xiao, Cloning, characterization, and production of three α-L-fucosidases from *Clostridium perfringens* ATCC 13124, J. Basic Microbiol. 56 (2016) 347-357.

[20] H. Ashida, A. Miyake, M. Kiyohara, J. Wada, E. Yoshida, H. Kumagai, T. Katayama, K. Yamamoto, Two distinct α-L-fucosidases from *Bifidobacterium bifidum* are essential for the utilization of fucosylated milk oligosaccharides and glycoconjugates, Glycobiology 19 (2009) 1010-1017.

[21] A. Pfenninger, M. Karas, B. Finke, B. Stahl, Structural analysis of underivatized neutral human milk oligosaccharides in the negative ion mode by nano-electrospray MS^n (Part 1: Methodology), J. Am. Soc. Mass Spectrom. 13 (2002) 1331-1340.

[22] H. Sakurama, S. Fushinobu, M. Hidaka, E. Yoshida, Y. Honda, H. Ashida, M. Kitaoka, H. Kumagai, K. Yamamoto, T. Katayama, 1,3-1,4-α-L-fucosynthase that specifically introduces Lewis a/x antigens into type-1/2 chains, J. Biol. Chem. 287 (2012) 16709-16719.

[23] L. Guillotin, P. Lafite, R. Daniellou, Unraveling the substrate recognition mechanism and specificity of the unusual glycosyl hydrolase family 29 BT2192 from *Bacteroides thetaiotaomicron*, Biochemistry 53 (2014) 1447-1455.

[24] M.J. Baumann, J.M. Eklöf, G. Michel, A.M. Kallas, T.T. Teeri, M. Czjzek, H. Brumer, Structural evidence for the evolution of xyloglucanase activity from xyloglucan endo-transglycosylases: biological implications for cell wall metabolism, Plant Cell. 19 (2007) 1947-1963.

[25] L. Beier, A. Svendsen, C. Andersen, T.P. Frandsen, T.V. Borchert, J.R. Cherry, Conversion of the maltogenic α-amylase Novamyl into a CGTase, Protein Eng., Des. Sel. 13 (2000) 509-513.

[26] B. Bissaro, J. Durand, X. Biarnés, A. Planas, P. Monsan, M.J. O'Donohue, R. Fauré, Molecular design of non-Leloir furanose-transferring enzymes from an α-L-arabinofuranosidase: a rationale for the engineering of evolved transglycosylases, ACS Catal. 5 (2015) 4598-4611.

[27] B. Bissaro, P. Monsan, R. Fauré, M.J. O'Donohue, Glycosynthesis in a waterworld: new insight into the molecular basis of transglycosylation in retaining glycoside hydrolases, Biochem. J. 467 (2015) 17-35.

[28] D. Talens-Perales, J. Polaina, J. Marín-Navarro, Structural dissection of the active site of *Thermotoga maritima* β-galactosidase identifies key residues for transglycosylating activity, J. Agric. Food Chem. 64 (2016) 2917-2924.

[29] C. Nyffenegger, R.T. Nordvang, C. Jers, A.S. Meyer, J.D. Mikkelsen, Design of *Trypanosoma rangeli* sialidase mutants with improved trans-sialidase activity, PLOS One 12 (2017) e0171585.

[30] G. Osanjo, M. Dion, J. Drone, C. Solleux, V. Tran, C. Rabiller, C. Tellier, Directed evolution of the α-L-fucosidase from *Thermotoga maritima* into an α-L-transfucosidase, Biochemistry 46 (2007) 1022-1033.

[31] B.M. Nestl, B. Hauer, Engineering of flexible loops in enzymes, ACS Catal. 4 (2014) 3201-3211.

[32] E.L. Summers, C.D. Moon, R. Atua, V.L. Arcus, The structure of a glycoside hydrolase 29 family member from a rumen bacterium reveals unique, dual carbohydrate-binding domains, Acta Cryst. F72 (2016) 750-761.

[33] J.P. Richard, X. Zhai, M.M. Malabanan, Reflections on the catalytic power of a TIM-barrel, Bioorg. Chem. 57 (2014) 206-212.

[34] G. Davies, B. Henrissat, Structures and mechanisms of glycosyl hydrolases, Structure 3 (1995) 853-859.

[35] B. Höcker, C. Jürgens, M. Wilmanns, R. Sterner, Stability, catalytic versatility and evolution of the $(\beta\alpha)_8$-barrel fold, Curr. Opin. Biotechnol. 12 (2001) 376-381.

[36] A. Ochoa-Leyva, X. Soberón, F. Sánchez, M. Argüello, G. Montero-Morán, G. Saab-Rincón, Protein design through systematic catalytic loop exchange in the $(\beta/\alpha)_8$ fold, J. Mol. Biol. 387 (2009) 949-964.

[37] A. Ochoa-Leyva, F. Barona-Gómez, G. Saab-Rincón, K. Verdel-Aranda, F. Sánchez, X. Soberón, Exploring the structure-function loop adaptability of a $(\beta/\alpha)_8$-barrel enzyme through loop swapping and hinge variability, J. Mol. Biol. 411 (2011) 143-157.

[38] R.T. Nordvang, C. Nyffenegger, J. Holck, C. Jers, B. Zeuner, U.K. Sundekilde, A.S. Meyer, J.D. Mikkelsen, It all starts with a sandwich: Identification of sialidases with trans-glycosylation activity, PLOS One 11 (2016) e0158434.

[39] A. Buschiazzo, M.F. Amaya, M.L. Cremona, A.C. Frasch, P.M. Alzari, The crystal structure and mode of action of trans-sialidase, a key enzyme in *Trypanosoma cruzi* pathogenesis, Mol. Cell. 10 (2002) 757-768.

[40] T. Kuriki, H. Kaneko, M. Yanase, H. Takata, J. Shimada, S. Handa, T. Takada, H. Umeyama, S. Okada, Controlling substrate preference and transglycosylation activity of neopullulanase by manipulating steric constraint and hydrophobicity in active center, J. Biol. Chem. 271 (1996) 17321-17329.

[41] P. Lundemo, P. Adlercreutz, E.N. Karlsson, Improved transferase/hydrolase ratio through rational design of a family 1 β-glucosidase from *Thermotoga neapolitana*, Appl. Environ. Microbiol. 79 (2013) 3400-3405.

[42] M.A. Frutuoso, S.R. Marana, A single amino acid residue determines the ratio of hydrolysis to transglycosylation catalyzed by β-glucosidases, Protein Pept. Lett. 20 (2013) 102-106.

[43] V. Ginsburg, D.A. Zopf, K. Yamashita, A. Kobata, Oligosaccharides of human milk: isolation of a new pentasaccharide, lacto-N-fucopentaose V, Arch. Biochem. Biophys. 175 (1976) 565-568.

[44] M. Okuyama, K. Matsunaga, K. Watanabe, K. Yamashita, T. Tagami, A. Kikuchi, M. Ma, P. Klahan, H. Mori, M. Yao, A. Kimura, Efficient synthesis of α-galactosyl oligosaccharides using a mutant *Bacteroides thetaiotaomicron* retaining α-galactosidase (*Bt*GH97b), FEBS J. 284 (2017) 766-783.

[45] D. Huang, K. Yang, J. Liu, Y. Xu, Y. Wang, R. Wang, B. Liu, L. Feng, Metabolic engineering of *Escherichia coli* for the production of 2'-fucosyllactose and 3-fucosyllactose through modular pathway enhancement, Metab. Eng. 41 (2017) 23-38.

[46] B. Priem, M. Gilbert, W.W. Wakarchuk, A. Heyraud, E. Samain, A new fermentation process allows large-scale production of human milk oligosaccharides by metabolically engineered bacteria, Glycobiology 12 (2002) 235-240.

[47] F. Baumgärtner, G.A. Sprenger, C. Albermann, Galactose-limited fed-batch cultivation of *Escherichia coli* for the production of lacto-*N*-tetraose, Enzyme Microb. Technol. 75-76 (2015) 37-43.

[48] F. Baumgärtner, L. Jurzitza, J. Conrad, E. Beifuss, G.A. Sprenger, C. Albermann, Synthesis of fucosylated lacto-*N*-tetraose using whole-cell biotransformation, Bioorg. Med. Chem. 23 (2015) 6799-6806.

[49] C. Dumon, E. Samain, B. Priem, Assessment of the two *Helicobacter pylori* α-1,3-fucosyltransferase ortholog genes for the large-scale synthesis of LewisX human milk oligosaccharides by metabolically engineered *Escherichia coli*, Biotechnol. Prog. 20 (2004) 412-419.

Figure legends

Figure 1. Transfucosylation reactions catalysed by α-L-1,3/4-fucosidases. Top: Formation of lacto-*N*-fucopentaose II (LNFP II) from 3-fucosyllactose (3FL) and lacto-*N*-tetraose (LNT). Bottom: Formation of LNFP III from 3FL and lacto-*N*-neotetraose (LNnT). The fucosyl moieties are shown in blue.

Figure 2. Homology model of *Bb*AfcB (white) indicating the catalytic residues D703 and E746 (yellow). The ligand comprising Fuc (orange), GlcNAc, and non-reducing end Gal (purple-blue) moieties from LNFP II is from the crystal structure of *Bi*AfcB (PDB: 3UET). The *Bb*AfcB α-helical loop (759-AAYNDGVDKVSLKPGQMAPDGKL-781) subjected to mutation in the current work is shown in black. The position and shape of corresponding α-helical loop (259-DIEKMKERENPTYLNNG-275) in the *Cp*Afc2 homology model to which it was changed is indicated in pink.

Figure 3. Transfucosylation catalysed by the α-L-1,3/4-fucosidases. Molar transfucosylation yields ([LNFP II/III]/$[3FL]_0$) obtained in transfucosylation catalysed by *Bb*$AfcB_{mut}$ (squares), *Bb*AfcB (triangles), and *Cp*Afc2 (circles) using 3FL as fucosyl donor substrate and either LNT (left) or LNnT (right) as acceptor substrate (*n* = 2). Acceptor-to-donor ratios (A:D) were either 10 (10 mM 3FL and 100 mM LNT/LNnT; filled symbols) or 1 (20 mM of both substrates; open symbols).

Figure 4. Effect of acceptor-to-donor ratio (A:D) and substrate concentration on transfucosylation. The reaction was catalysed by *Bb*$AfcB_{mut}$ (squares) and *Bb*AfcB (triangles) for up to 60 min using 3FL and LNT (*n* = 2). For A:D 1 and 5 (dashed lines) the 3FL donor concentration was 20 mM, whereas it was 10 mM for A:D 2 and 10 (solid lines). For A:D 1 and 2 (open symbols) the LNT acceptor concentration was 20 mM, whereas it was 100 mM for A:D 5 and 10 (filled symbols). Transfucosylation activity is given as molar LNFP II yield on donor (%; left) and as LNFP II concentration (mM; right).

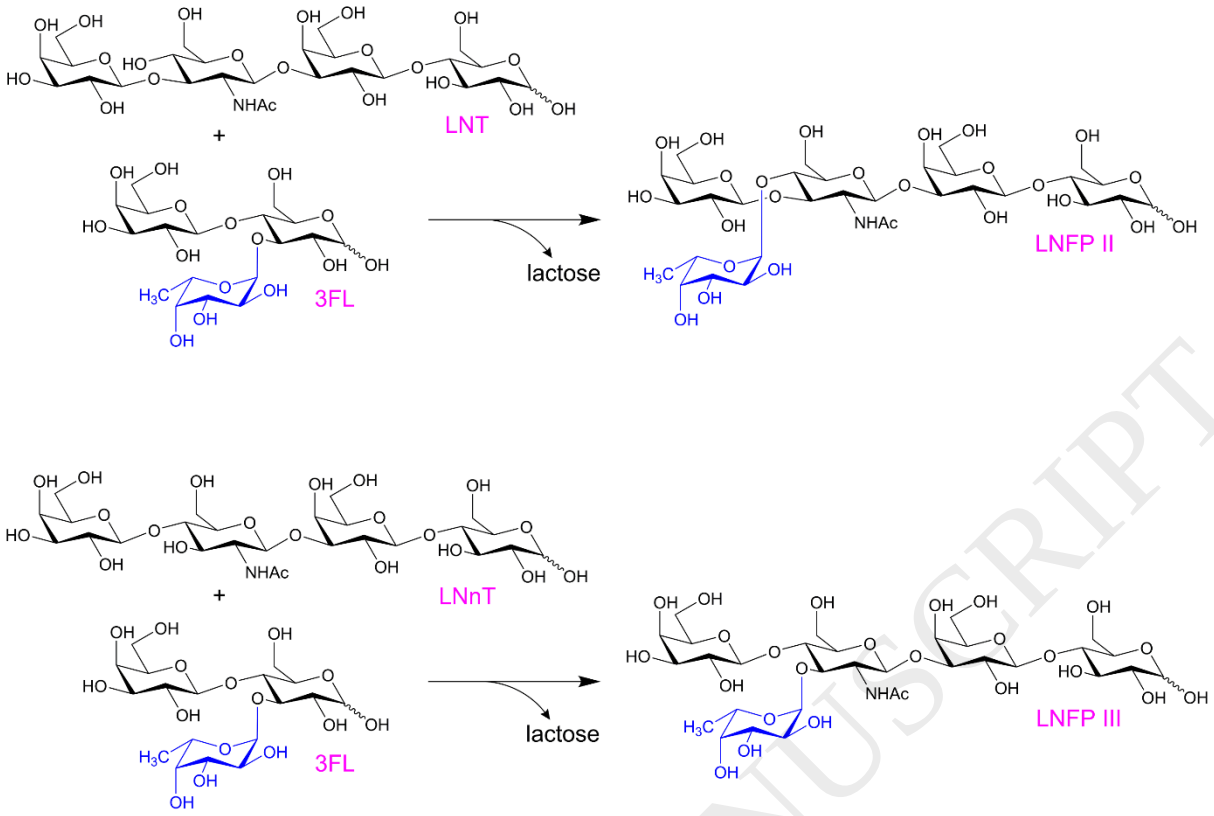

Figure 1.

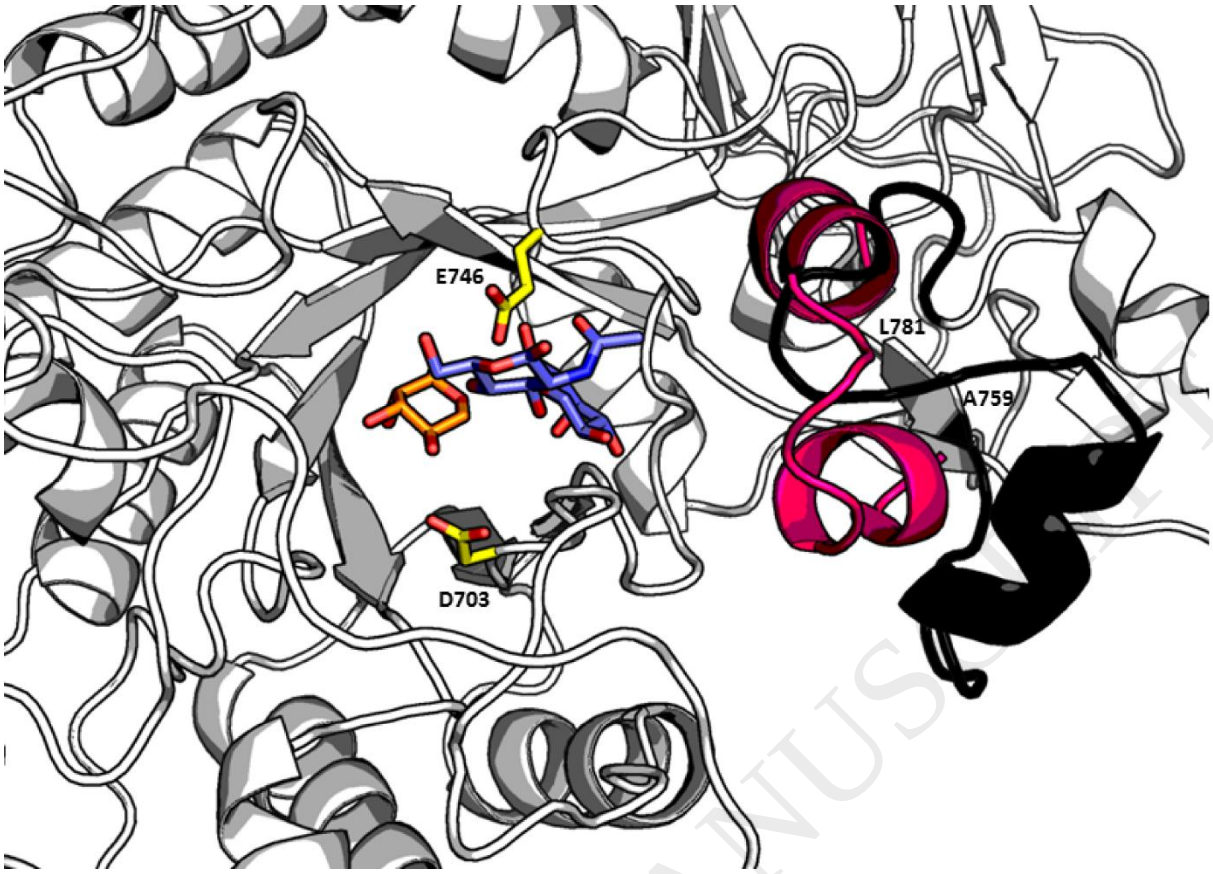

Figure 2.

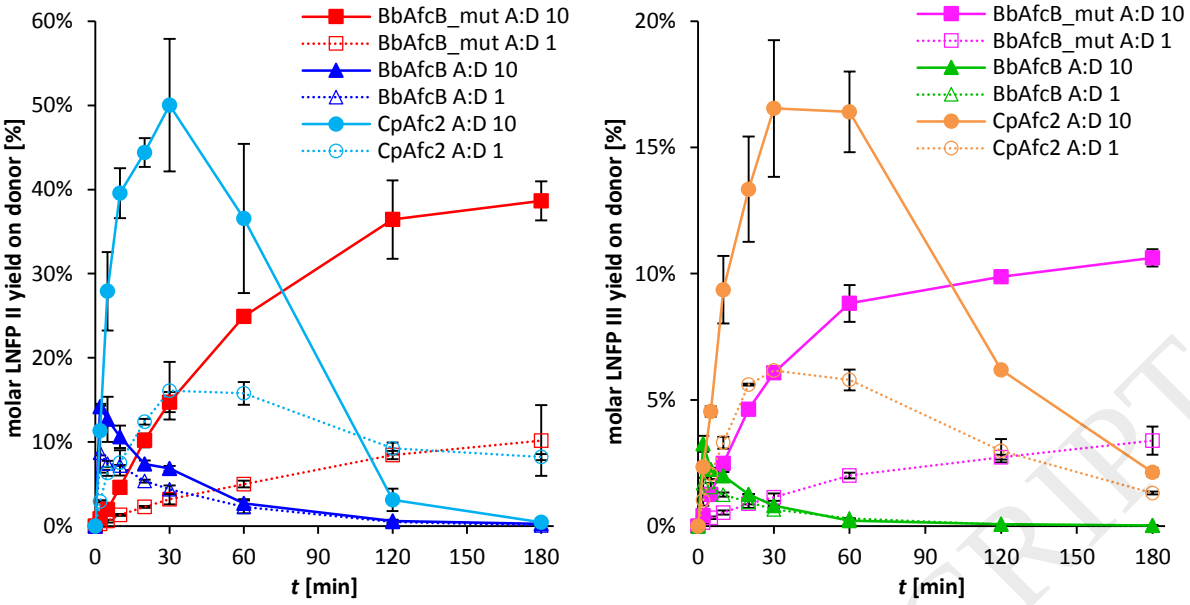

Figure 3.

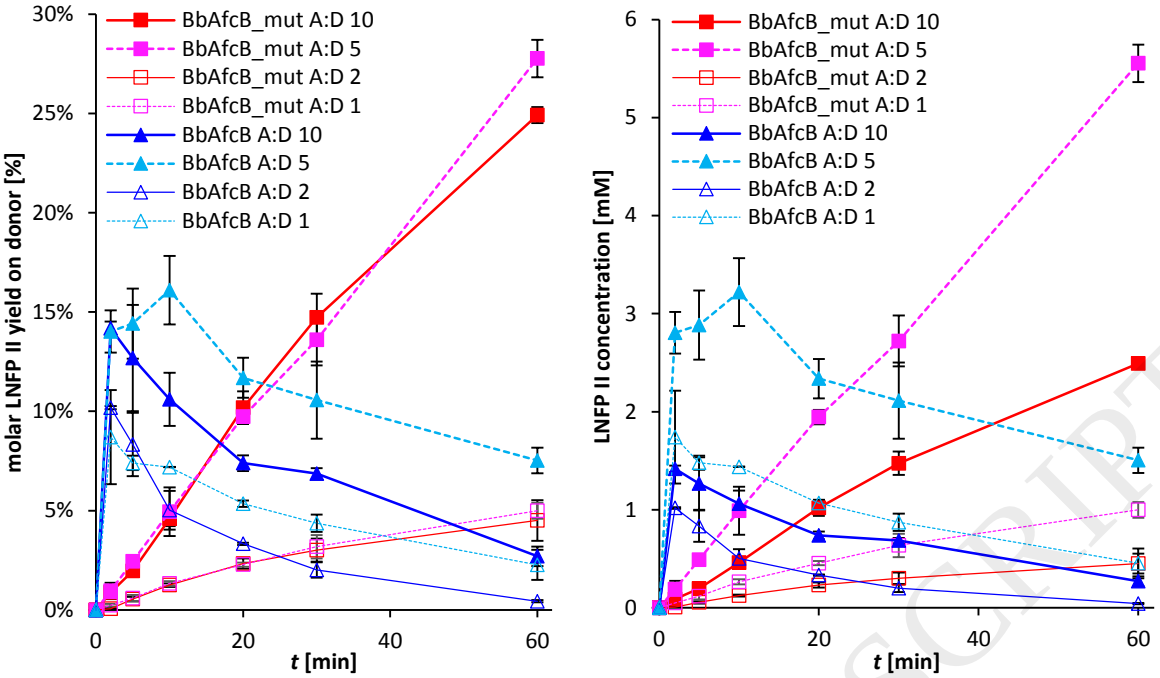

Figure 4.

Tables

Table 1. Hydrolytic activity of α-1,3/4-L-fucosidases on 3FL (n = 2).

Enzyme	**Hydrolytic activity on 3FL** (μmol min^{-1} (μmol enzyme)$^{-1}$)
*Cp*Afc2	18 ± 3[b]
*Bb*AfcB	59 ± 1.5[a]
*Bb*AfcB$_{mut}$	0.01 ± 0.001[c]

[a-c]Significant difference (p < 0.05) between enzymes.

Table 2. Initial transfucosylation rate, maximum conversion yield ([LNFP II/III]/[3FL]$_0$), and yield after 24 hours in transfucosylation catalysed by *Bb*AfcB, *Bb*AfcB$_{mut}$, and *Cp*Afc2 using 3FL as donor substrate and either LNT or LNnT as acceptor substrate (n = 2) at acceptor-to-donor ratios (A:D) of either 10 or 1.

Acceptor	Enzyme	A:D	3FL (mM)	Initial transfucosylation rate (μM min^{-1})	Maximum yield of LNFP II/III (% (mM))	LNFP II/III yield after 24 hours (%)
LNT	***Bb*AfcB$_{mut}$**	10	10	$46 \pm 6^{d,x}$	$39 \pm 2^{b,x}$ (3.9)	34 ± 11
		1	20	$24 \pm 4^{d,y}$	$13 \pm 4^{c,y}$ (2.7)	13 ± 4
	***Bb*AfcB**	10	10	$709 \pm 17^{ab,x}$	$14 \pm 0.3^{c,x}$ (1.4)	0.7 ± 0.04*
		1	20	$870 \pm 237^{a,x}$	$8.7 \pm 2^{c,y}$ (1.7)	0.4 ± 0.1*
	***Cp*Afc2**	10	10	$517 \pm 56^{bc,x}$	$50 \pm 8^{a,x}$ (5.0)	0.8 ± 0.8*
		1	20	$273 \pm 0.3^{cd,y}$	$16 \pm 3^{c,y}$ (3.2)	0.4 ± 0.6*
LNnT	***Bb*AfcB$_{mut}$**	10	10	$23 \pm 2^{c,y}$	$11 \pm 0.3^{b,y}$ (1.1)	5.4 ± 2*
		1	20	$12 \pm 2^{c,z}$	$8.1^{bc,y}$ (1.6)	8.1
	***Bb*AfcB**	10	10	$163 \pm 16^{a,y}$	$3.3 \pm 0.3^{d,z}$ (0.3)	0.1 ± 0.02*
		1	20	$169 \pm 22^{a,y}$	$1.7 \pm 0.2^{d,z}$ (0.3)	0*
	***Cp*Afc2**	10	10	$101 \pm 5^{b,z}$	$17 \pm 3^{a,y}$ (1.7)	0.1 ± 0.03*
		1	20	$77 \pm 6^{b,z}$	$6.2 \pm 0.2^{c,y}$ (1.2)	0.04 ± 0.002*

[a-d]Significant difference (p < 0.05) between values for each parameter comparing enzymes on the same acceptor substrate (LNT or LNnT) at both A:Ds. [x-z]Significant difference (p < 0.05) between values for each parameter comparing acceptor substrates for the same enzyme at both A:Ds. *For yields after 24 hours, an asterisk indicates whether this value is significantly different from the maximum yield, i.e. if significant product hydrolysis took place within 24 hours.

Table 3. Effect of acceptor-to-donor ratio (A:D) and substrate concentrations on initial transfucosylation rate (divided by [3FL]$_0$ to clearly observe the effect of varying donor and acceptor concentrations) and on maximum LNFP II yield (given as molar yield on donor, i.e. [LNFP II]/[3FL]$_0$) obtained within 60 min in the transfucosylation catalysed by *Bb*AfcB, *Bb*AfcB$_{mut}$, and *Cp*Afc2 using 3FL and LNT (n = 2).

A:D	3FL (mM)	LNT (mM)	Initial transfucosylation rate (μM min^{-1} (mM 3FL$_0$)$^{-1}$)			Maximum LNFP II yield in 60 min (mM (mM 3FL$_0$)$^{-1}$)		
			***Bb*AfcB$_{mut}$**	***Bb*AfcB**	***Cp*Afc2**	***Bb*AfcB$_{mut}$**	***Bb*AfcB**	***Cp*Afc2**
1	20	20	1.2 ± 0.2^{d}	44 ± 12^{b}	14 ± 0.0^{c}	0.05 ± 0.004^{e}	0.09 ± 0.02^{de}	0.17 ± 0.03^{c}
2	10	20	1.2 ± 0.1^{d}	51 ± 0.4^{b}	-	0.05 ± 0.01^{e}	0.10 ± 0.001^{d}	-
5	20	100	4.8 ± 0.2^{cd}	70 ± 5.3^{a}	-	0.28 ± 0.01^{b}	0.16 ± 0.02^{c}	-
10	10	100	4.6 ± 0.6^{cd}	71 ± 1.7^{a}	52 ± 5.6^{b}	0.25 ± 0.004^{b}	0.15 ± 0.001^{cd}	0.51 ± 0.07^{a}

[a-d]Significant difference ($p < 0.05$) between values for each parameter.